Optimization of Mesoporous Silica Nanoparticles of Silymarin through Statistical Design Experiment and Surface Modification by APTES

Sheetal B. Gosavi* and Moreshwar P. Patil

Department of Pharmaceutics, MET's Institute of Pharmacy, Affiliated to Savitribai Phule, Pune University, Adgaon, Nashik, MH, India.

The major goal of this study was to create surface-modified mesoporous silica nanoparticles (MSN) of Silymarin, which has a short half-life and requires regular dosing due to first-pass metabolism. MSN was prepared by cost effective Sol-Gel method, functionalized by (3-Aminoprpyl) triethoxysilane (3-APTES). Evaluated and compared the Silymarin-loaded MSN and APTES functionalized MSN for drug loading, in-vitro dissolution, particle size, surface morphology, surface area, pore size and volume. The percent drug loading and encapsulation efficiency of APTES-functionalized MSN were found to be 92.50±0.72 % percent and 93.20±0.13 %, respectively, which showed a higher value in APTES-functionalized MSN as compared to Silymarin-loaded MSN. Drug release of APTES-functionalized MSN was 92.15 0.03%, which was more as compared to silymarin-loaded MSN. XRD showed that after functionalization silymarin changed from crystalline to amorphous form. SEM indicates that MSN was formed in a spherical shape with particle size of 196.7nm. The BET analysis proved that the nanoparticles had a larger surface area, which was reduced after drug loading and functionalization. Also, the pore size was increased and the pore volume was reduced after functionalization, indicating the incorporation of silymarin. The results suggested that the functionalization might successfully increase adsorption capacity, larger surface area, and increased encapsulation. Mesoporous silica nanoparticles also showed a greater impact on dissolution.

Keywords: APTES; Dissolution; Functionalization; Mesoporous Silica Nanoparticles; Silymarin; Sol-gel Process.

Biopharmaceuticals are now known for their limited water solubility. Solubility issues affect around 40% of drugs approved for market and 60% of drugs in the development pipeline. Many drugs confront substantial hurdles in clinical use due to their low water solubility, preventing them from adopting a formulation strategy capable of producing large loads and rapid dissolving rates.[1,2] Oral medication delivery is the simplest and most convenient method of drug administration. However, the bulk of new medications originating from drug discovery programs demonstrate relatively poor water solubility, resulting in poor oral bioavailability due to inadequate dissolution throughout the gastrointestinal tract.[3,4] In recent decades, several researches have been conducted to address this issue. [5] The challenge facing formulation scientists working on novel drug

*Corresponding author E-mail: sheetalgosavi28@gail.com

candidates for oral delivery is coming up with plans to get around this obstacle and enable oral administration of these novel medicines.[6-8] MCM-41 is a mesoporous silica material that was first described in 2001 as a medication delivery device. Because of their textural characteristics, which raise the loading amount of drugs inside the pore channels, mesoporous silica materials have been proposed to be good drug delivery carriers. Likewise, the functionalization of the silanol group allows for the regulation of drug diffusion kinetics.[9-11] Mesoporous silica materials offer several advantageous qualities, including a wide surface area, easily adjustable pore size and volume, chemical inertness, and ease of surface chemical functionalization.[12-24]

It is crucial to create unique MSNs and medication combinations in a way that promotes better dissolving in order to solve these issues.[25] Using cetyltrimethylammonium bromide (CTAB) as a surfactant and tetraethyl orthosilicate (TEOS) as an alkoxide precursor, mesoporous silica nanoparticles (MSNs) were synthesised via the sol-gel method. The amount of surfactant in the particle has a significant impact on its morphology, which can change from distributed nanospheres to agglomerates. This can affect TEOS hydrolysis and CTAB micelization.[26] In contrast, unaltered MSNs have just Groups of silanol on the walls of the pore channels, which establish flimsy hydrogen bonds with the experimental drug. As a result, they are insufficiently powerful to store the medication and allow for its continuous release.[27-28] Efforts have been undertaken to introduce functional groups to the pore channel walls in anticipation of their potential usage in sustained drug delivery applications. This work aimed to improve the drug loading capacity and dissolution rate by loading a weakly water-soluble medicine into MSN for oral administration. In order to do this, the influence of different MSN surface chemical groups and pore diameters (particle size of under 100 nanometers). Using SEM, nitrogen adsorption, XRD, FT-IR, and DSC, the absorption and release of the model drug Silymarin were thoroughly examined.[29] Silymarin has minimal aqueous solubility and poor penetration throughout the intestinal fluid. Furthermore, silymarin is vulnerable to breakdown by intestinal juices. Such shortcomings have led to slow dissolution rates and inadequate oral bioavailability.[30]

In this study MSN was functionalized with 3 aminopropyltriethoxysilane (3-APTES-SLM) i.e. amino functionalization to investigate the drug loading and drug release. The amount of template and stirring speed were examined in this study using a Central Composite design. The criterion for batch optimization was higher drug release and lower particle size.

EXPERIMENTAL DETAILS

Materials

Silymarin was purchased from Yucca laboratories, Mumbai, tetraethyl ortho silicate, cetyltrimethyl ammonium bromide were purchased from Siga Aldrich, (3-Aminopropyl) triethoxysilane was purchased from Tokyo Chemical Laboratory, Tokyo, Japan. Ammonia solution and alcohol obtained from SD Fine Chemicals Mumbai

Preparation of MSN

Silica solution was made by combining 20Mol ethanol, 45.6Mol water, and an 10.4Mol ammonia solution. After 15 minutes of stirring, CTAB of various concentrations which is mentioned in table 2 was added to the original mixture. After that, the TEOS 1Mol was added drop by drop while being constantly stirred for two hours at room temperature. The solution became opaque very quickly, suggesting that the reaction had begun. After precipitating, the white powder was filtered and then washed with deionized water. Overnight, the particles were left to dry at room temperature. To get rid of the surfactant, the particles were calcined at 550°C for four hours.[31] Finally, blank MSN were prepared as shown in Scheme 1.

Optimization of MSN

The central composite design was employed to optimize the MSN. With Design Expert 7.0, the central composite's experimental design and statistical analysis were completed. The CC was created to include two factors and two responses, as indicated in table 1. Through CC, several values were developed, and an optimum response was fitted to a quadratic, 2Fi, or linear model. The model offered for each response was examined using ANOVA. It was validated using characteristics such as the luck of p-value, the

squared correlation coefficient (R^2), and precision. Consequently, a statistical model was used to construct MSN with optimal response values.

Amino Functionalization

The produced blank MSNs were functionalized with aminopropyl groups via a post-synthesis method depicted in Scheme 1. The generated blank MSNs of 0.5g were dispersed in 20 mL of ethanol using an ultrasonic bath for 20 minutes. The APTES was promptly added and mixed at 500 rpm for 3 hours at room temperature in varying concentrations of 0.5%, 1%, 1.5%, and 2%. The APTES-MSNs were separated by centrifugation (REMI, Mumbai) at 7000 rpm for 5 minutes. It was cleaned three times with ethanol before being let to dry overnight at room temperature.

Drug Loading

The drug was loaded into mesoporous silica nanoparticles using the solvent immersion technique. Ethanol is utilized as a solvent to load drugs into MSNs. If the concentration is too high, drug molecules quickly adsorb onto the surface and clog the mesopores, decreasing the accessible surface area for medication loading. Drug and APTES-MSN were mixed in 10 mL of ethanol at a 1:1 ratio. The solution is then collected and centrifuged for 5 minutes. The supernatant is discarded, and mesoporous silica nanoparticles are collected and dried at room temperature for up to 24 hours. These mesoporous silica nanoparticles were evaluated for percent yield, drug loading capacity, and entrapment efficiency.[32] The drug loading and entrapment efficiency were determined using the method shown schematically in Scheme 2.

Entrapment Efficiency % = [Total amount of drug in MSNs / Total weight of sample] × 100

Drug Loading Capacity % =[Total amount of drug in MSNs / Total amount of drug initially added] × 100

Characterization

Morphology of SLM-MSNs and SLM-APTES-MSNs

The morphology and form of synthesized MSN were studied using SEM (Hitachi SU 1510) at a voltage of 15 kV. The MSN samples were coated on an aluminum stub with double-sided adhesive carbon tape and gold using an MC1000 ion sputtering system.

Nitrogen adsorption and isotherm by BET

The generated MSN's surface area, pore size, and pore volume were measured using the nitrogen adsorption/desorption isotherm for eight hours at 300ºC under vacuum at -196.14ºC using a Quantachrome Nova station instrument, version 11.05 analyzer. The samples were outgassed at 150ºC for six hours prior to analysis. The specific surface area (SBET) was calculated with the Brauner-Emmett-Teller (BET) theory and multi-point adsorption data from a linear segment of the N2 adsorption isotherms. The pore volume and pore size distribution from the adsorption isotherms were calculated using non-local density functional theory.[29]

XRD, FTIR, DSC

The XRD pattern of the samples was acquired using a Brucker Axs diffractometer from Germany. The X-ray generator range at 40 kV and 30 mA, with the CuKå line at 1.54060 A as the radiation source. The samples were scanned at 250ºC from 100 to 800 (2è). FT-IR spectrometer (Shimadzu Co., Japan) was used to obtain the FT-IR spectra of the manufactured MSN and drug-loaded nanoparticles. Using absorbance mode, IR spectra were acquired between 400 and 4000 cm"1. Samples underwent thermal analysis using a DSC apparatus. The sample was maintained at the beginning temperature for 5 minutes and then heated from 30-350ÚC at a rate of 10ÚC/min while subjected to an extra dry nitrogen gas purge (20 mL/min).

Particle Size and Zeta Potential of MSN

The most essential physical attribute of a particle sample is particle size, which has a crucial significance in nanoparticles. The Malvern Zetasizer was used to determine the zeta potential and particle sizes. Approximately 5 mg of substance was diluted in distilled water and sonicated for five minutes. The prepared suspension was measured using Malvern Zetasizer.

In vitro dissolution

The TDT-08 dissolution tester from Electrolab Mumbai was used to conduct dissolution experiments utilizing a USP II paddle technique (50 rpm, 37±0.5 ÚC, and 900 mL dissolving media). The amount Silymarin loaded MSN as well as

functionalized MSN of various concentration of APTES taken Equivalent to 100 mg of Silymarin and exposed to dissolving medium at P^H of 6.8. Aliquots of 10mL were withdrawn at regular intervals, and a fresh volume of dissolving medium was added to maintain the constant dissolution volume. The samples were analyzed using a UV spectrophotometer (1800, Shimadzu Co., Japan) at 287 nm. The acquired data was fitted to several kinetic models, and the best match was selected.[33]

RESULTS AND DISCUSSION

Optimization of MSN

Using Design-Expert® 7.0 Software, an optimized MSN was created using central composite statistical analysis to determine the relationship between the proposed model and the response (Table 2). Particle size (Y1) and drug release (Y2) were critical responses in optimizing MSN. The rationale for each response choice is as follows. The particle size changes with the
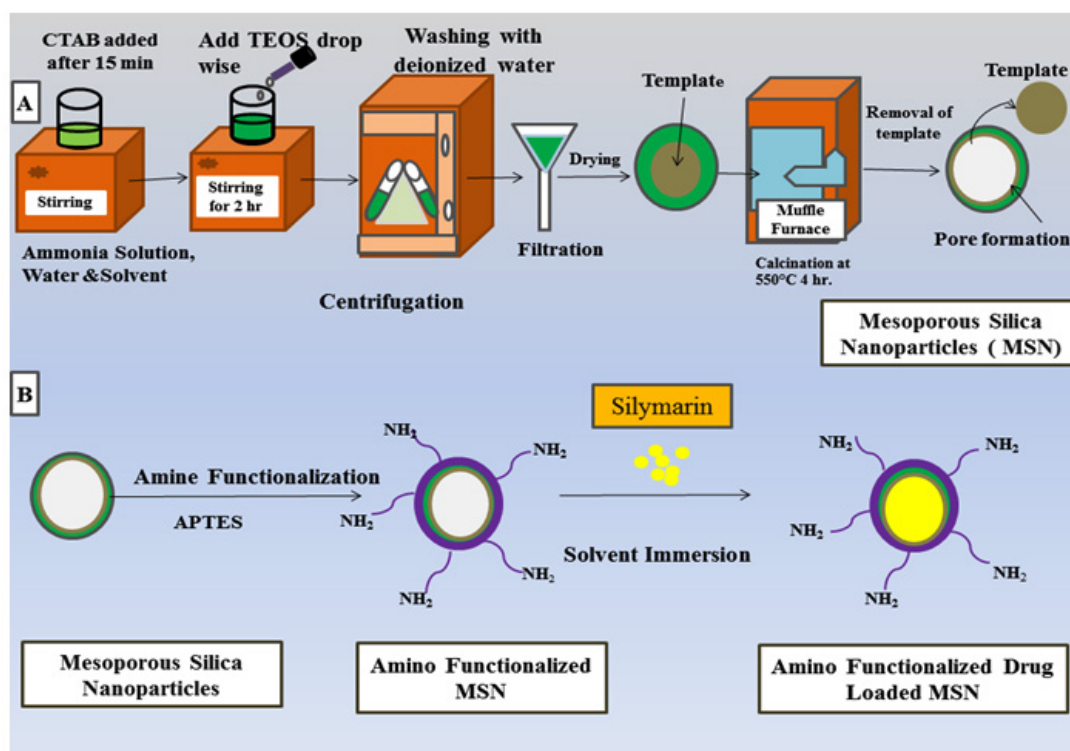
Scheme 1. Schematic illustration of A) Synthesis of Mesoporous Silica Nanoparticles B) Amino functionalization and drug loading

Scheme 2. Schematic representation of Drug loading by solvent immersion method

concentration of CTAB. As the concentration of CTAB (X1) rose, the particle size was reduced. Agglomeration of silica particles was found at low CTAB concentrations. At greater concentrations, the silica mesoporous structure grows via the Ostwald ripening mechanism. CTAB has a crucial role in agglomeration formation and TEOS hydrolysis. As the quantity of CTAB increases, so does the particle size. According to the literature, the amount of surfactant used impacts its hydrolysis and micellization. According to the study, when the stirring speed (X2) increases, the particle size decreases. The rate of drug release decreases as

the size of nanoparticles decreases. For successful medication release tests, minimum-sized MSNs with maximal drug release were used. The optimal formulation had 0.2Mol and 600 RPM of X1 and X2, respectively. Optimized MSN created uniform minimum particle size of 264nm (Y1) with high drug release of 79% (Y2) as shown in Table 2.

Surface Morphology

SEM images of blank MSN, silymarin loaded MSN and Amino functionalized silymarin loaded MSN shown on Fig. 2. In Figure 2A, it was observed that the porous and uneven nature of blank MSN. In figure 2B, the porous, uneven nature and shows an aggregation of silymarin loaded MSNs. In figure 2C, after surface functionalization it was observed that the porous nature of MSN shows no aggregation.

Nitrogen adsorption and isotherm by BET

Assuming pores are filled with liquid adsorbate, the amount of vapor adsorbed at a temperature near unity is used to compute the pore volume. The pore volume is used to assess the average pore size. Nitrogen adsorption and desorption isotherms of blank, silymarin loaded MSNs, surface functionalized silymarin loaded

Table 1. Factors and response used in response surface design

Factor	Response Surface Design	
	Low Limit	High Limit
X_1: CTAB	0.1M	0.5M
X_2: Stirring Speed	400	600
Response	Goal	
Y_1: Particle Size	Minimize	
Y_2: Drug Release	Maximize	

Table 2. Design of observation response and experiment setup. The values (n = 3) are shown as means SD

Run	Factor		Response	
	X_1 CTAB (Mol)	X_2 Stirring Speed(RPM)	Y_1 Particles Size(nm)	Y_2 Drug Release(%)
1	0.30	500	312.00±2.44	64.66±4.35
2	0.50	400	439.66±1.23	45.33±4.35
3	0.30	600	282.00±±2.82	70.41±2.61
4	0.30	400	368.60±2.82	59.34±1.73
5	0.10	400	276.00±7.07	72.21±4.35
6	0.10	500	271.00±1.44	75.00±4.58
7	0.20	600	264.00±2.44	79.00±3.46
8	0.50	600	372.00±3.55	55.14±3.46
9	0.58	500	438.00±4.54	46.33±4.35

Table 3. An overview of the statistical analysis and model fitting

Response	Suggested Model	Sequential P value	Lack of fit P-value	R^2	Adj R^2	Pred R^2	Adequate Precision
X_1	Quadratic	0.0020	0.2272	0.9930	0.9814	0.9405	23.028
X_2	Linear	0.0001	0.8917	0.9916	0.9888	0.9782	42.747

MSNs particles are shown in Fig 3 A, B, C. Nitrogen adsorption-desorption isotherm of the blank MSN showed a type IV isotherm, associated with mesoporous materials. The initial loop indicates the mono-multilayer adsorption and the second loop indicates desorption. These adsorption isotherms confirm the porous nature of the Mesoporous silica nanoparticles. It was observed that the surface area as well as pore volume of the blank MSN was more as compared to the silymarin loaded MSN and surface functionalized silymarin loaded MSN. The blank nanoparticle has a smaller pore size than silymarin-loaded MSNs. The decrease in surface area and pore volume might be attributed to silymarin and APTES adsorption on blank MSN surfaces. Data on surface morphology
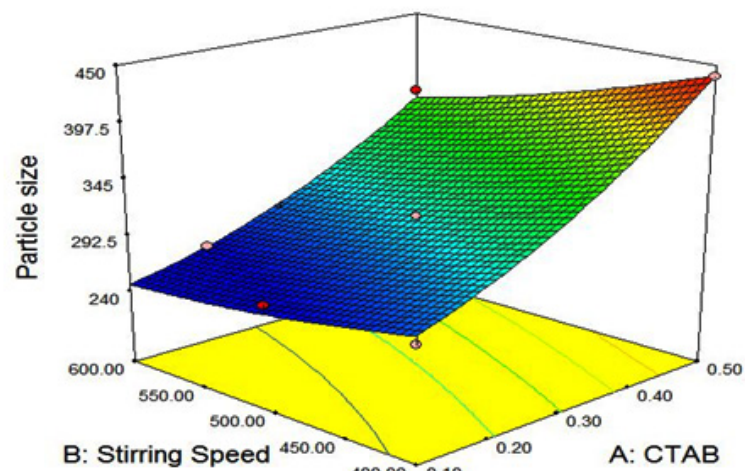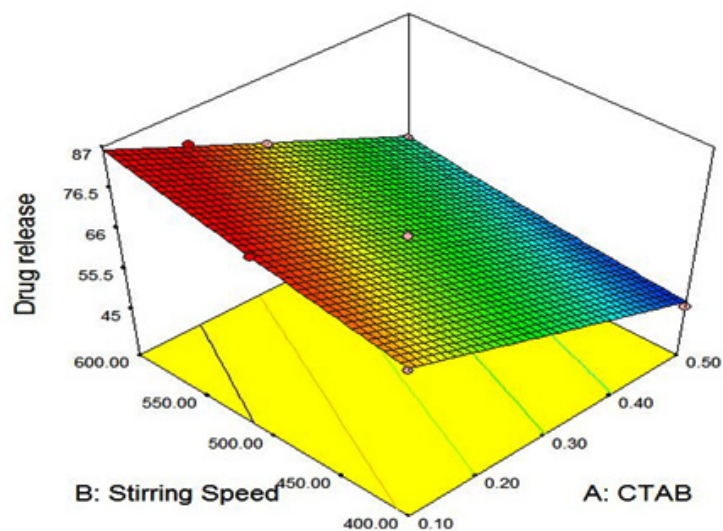

Fig. 1. Three-dimensional surface plot of A) Particle size) Drug release

and value are provided in Table 4.

XRD investigations, FTIR, and DSC data provide proof of MSN and AP-MSN impregnation

In Figure 4A XRD pattern of silymarin shows characteristic high intensity with prominent peaks of 2è value at 21Ú and 25Ú, which
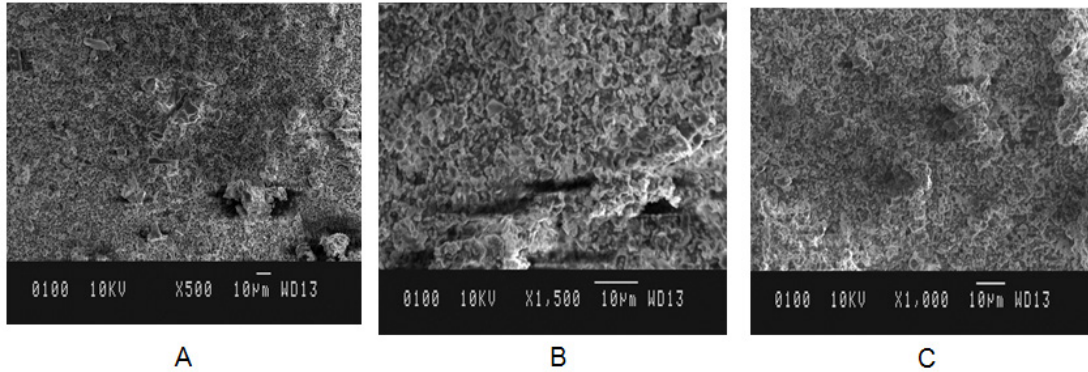

Fig. 2. Surface morphology of A) Blank MSN B) Silymarin Loaded MSN C) Amino functionalized Silymarin loaded MSN
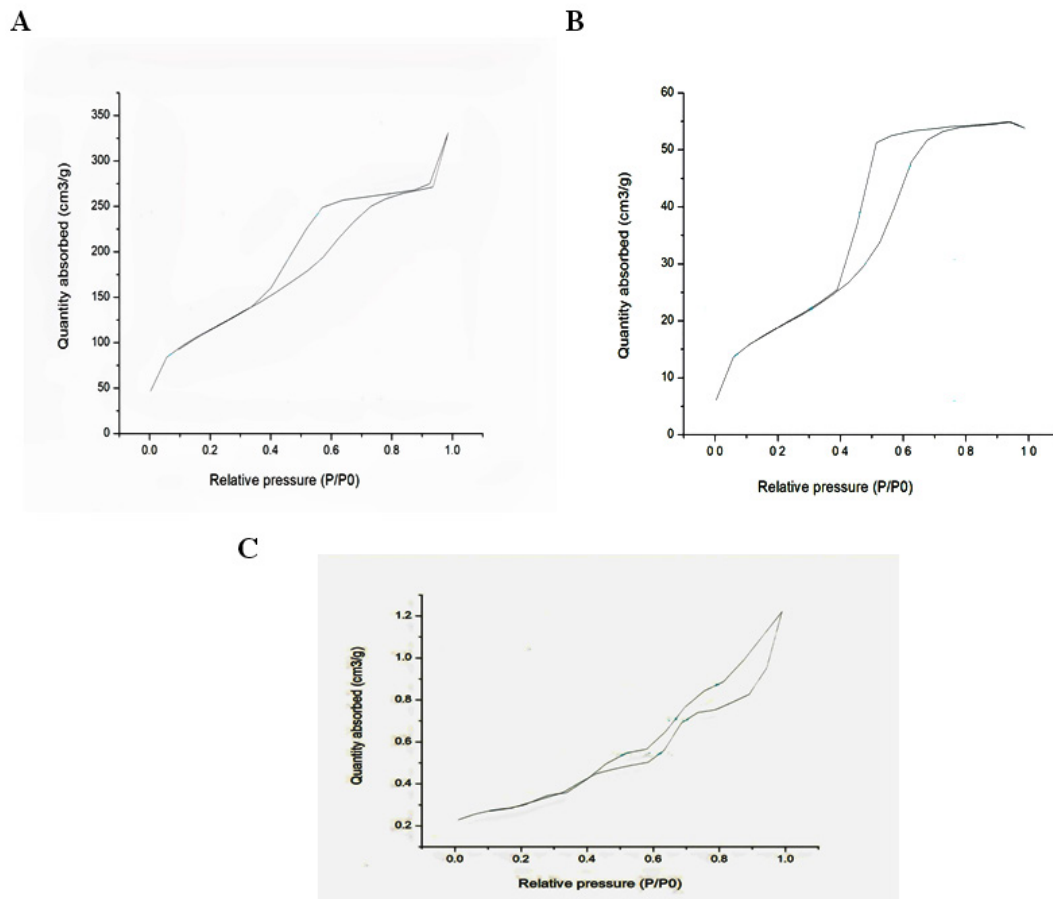

Fig. 3. N$_2$ Adsorption desorption A) Blank MSN B) Silymarin Loaded MSN C) APTES Functionalized Silymarin Loaded MSN

indicates that silymarin is present in crystalline form. In Figure 4B XRD pattern of silymarin loaded MSN shows the intensity of diffraction peaks was decreased, which shows the silymarin is successfully loaded into the blank MSNs. A very low- intensity peak 2è value at 24Úwas observed. In Figure 4C. XRD pattern of surface functionalized silymarin loaded MSNs shows that there is no present characteristics diffraction peaks which showed the functionalization of MSN surface by APTES molecules and confirmed that silymarin is present in amorphous form.

The IR spectrum of Silymarin and Silymarin loaded MSNs was determined in the range 400-4000 cm^{-1}. Fig.5 provided Blank MSN, Silymarin, Silymarin loaded MSN and Amino functionalized Silymarin loaded MSNs. The major IR peaks observed for Silymarin is 3439.08 (-OH), 2937.59 (-CH), 1639.49 (-C=O), 1230.58 (-C-O-C),1083.99 (-C-O) respectively. The Silymarin and Silymarin loaded MSN shows

similar peaks at the respective wave number. It was suggested that there is no chemical interaction between drugs and excipients. However, after surface functionalization, two new bands appear at 3148.44 (-NH$_2$) and 800.46 (-CH$_2$). Si-O-Si bonds are formed during surface functionalization by the reaction of hydroxyl groups with APTES. A method of anchoring involving an interaction between silanol groups and APTES is implied by the reduction in hydroxyl groups. There was a new band found at 1592 cm"1, which pointed to NH2 asymmetric bending.

The DSC thermogram of silymarin shown in Figure 6 suggested that it might be absorb moisture from the air, which shows deep endotherm at about 82ºC. The peak was observed at 147.16 ºC which corresponds to the melting point of silybin, an active constituent of silymarin complex. The weak endothermic peak at 260ºC, corresponds to the melting point of taxifolin and silychristin which is the active constituent of silymarin. In silymarin

Table 4. Surface area and porosity information for blank and drug-loaded mesoporous silica nanoparticles (MSN)

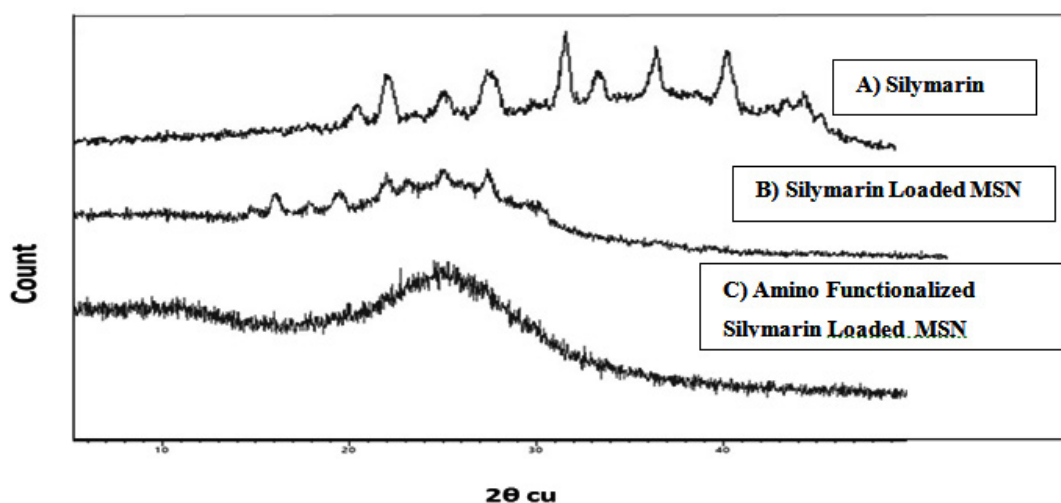| Sample Name	SBET(m^2/g)	Pore Size (nm)	Pore Volume (cm^3/g)
Blank MSNs	488.460	3.922	0.527
SLM-MSN	100.028	3.454	0.094
APTES-MSN	269.24	2.562	0.065
APTES-SLM-MSN	1.946	2.293	0.002

Fig. 4. XRD image for A. Silymarin   B. Silymarin Loaded MSN C. Amino Functionalized Silymarin Loaded MSN

loaded MSN, the melting endotherm was observed at 86.91°C and 147°C, which reveals the existence of drug in the MSN.

The complete disappearance of endothermic peak at 235°C as compared to silymarin; Thus it confirms that the presence of silymarin in amorphous state in MSNs. In surface functionalized silymarin loaded MSNs, the melting endotherm was observed at 82°C which was due to the silymarin absorbs moisture from the air. The complete disappearance of peak at 156.60°C as compared to silymarin loaded MSNs is due to condensation of surface silanol groups present in APTES at the same interval of melting temperature, which appears in silymarin loaded MSN; Thus it confirms that the presence of silymarin in an amorphous state in MSN.

%DL and %EE

By using various concentrations of APTES the Amino-functionalized MSNs were prepared and investigated for drug loading and entrapment efficiency. Drug loading and EE% were found for unmodified mesoporous silica nanoparticles were 88.90±1.62% and 67.50±0.76% optimized batch 93.20±0.13% and 92.50±0.72% respectively. For Amino-functionalized MSN these observations were found more as compared to the unmodified mesoporous silica nanoparticles.

Zeta potential and particle size

The zeta potential of blank MSN was

Table 5. Dissolution Kinetic data for Silymarin Loaded MSN

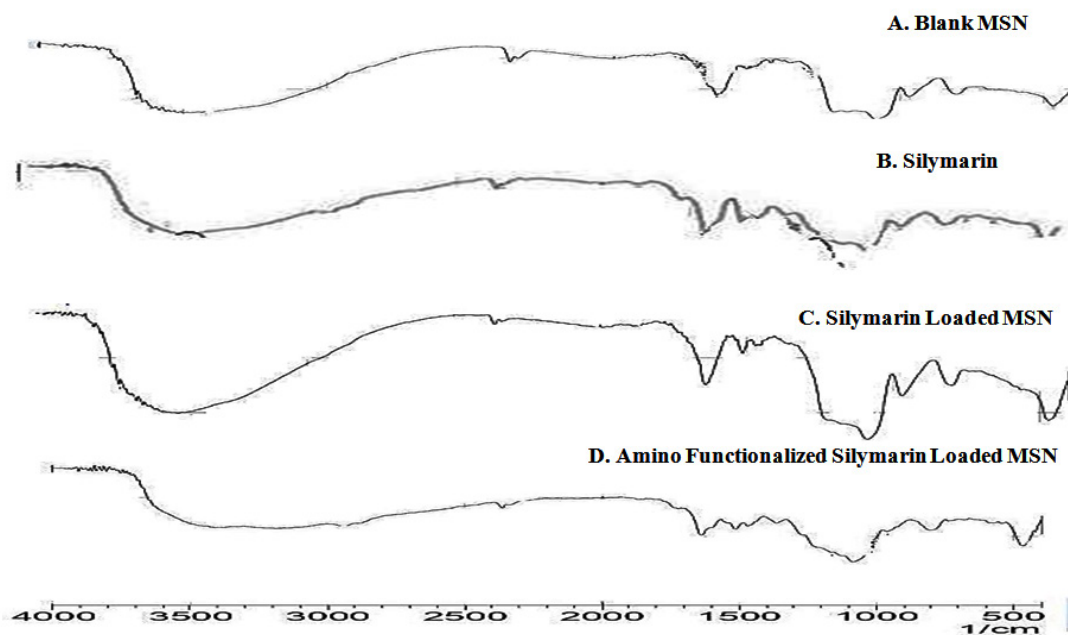| Formulation	Statistical Parameter	Dissolution Model				
		Zero	First	Higuchi	Hixson Crowell	Korsmeyer peppas
Silymarin	R^2	0.9984	0.9828	0.9889	0.9907	0.9984
Loaded	AIC	58.6869	74.78	84.67	64.98	42.85
MSN	MSC	4.0483	2.70	1.88	3.52	5.36

Fig. 5. FTIR for A. Blank MSN B. Silymarin C. Silymarin Loaded MSN D. Amino Functionalized Silymarin Loaded MSN

found -6.73, the negative value due to the -Si-O-H group present on the surface of MSN. The zeta potential of silymarin loaded MSN -19.1 because of surface hydroxyl groups (-OH) present in silymarin. The zeta potential of surface functionalized silymarin loaded MSN is -21.1 due to -Si-O2 and -NH2 groups present in APTES. This value of zeta potential suggested that the MSN has good stability by electrostatic repulsion. Particle size of blank MSN, silymarin loaded MSN, and surface functionalized silymarin loaded MSNs is detected at 263.2 nm, 210.1 nm and 196.7 nm

Table 6. Dissolution Kinetic data for APTES Functionalized Silymarin Loaded MSN

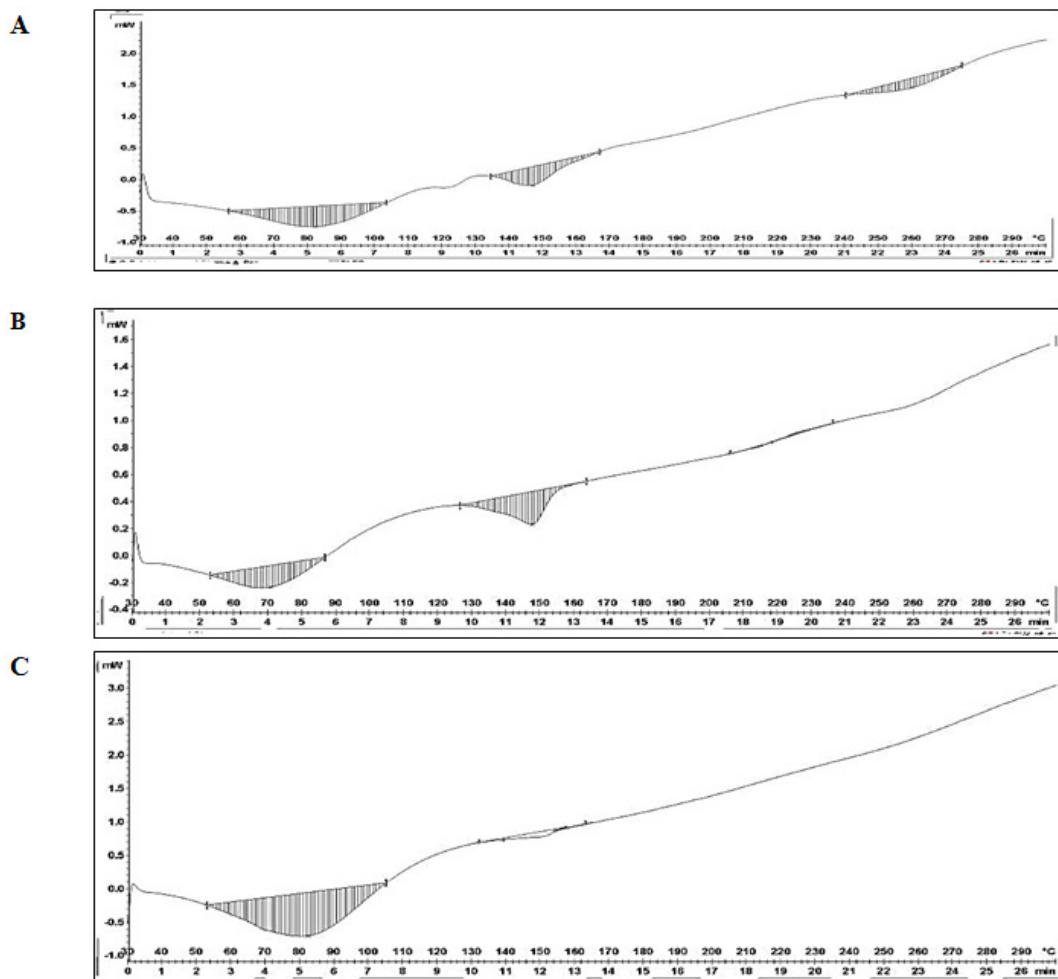| Formulation | Statistical Parameter | Dissolution Model | | | | |
		Zero	First	Higuchi	Hixson Crowell	Korsmeyer peppas
APTES	R^2	0.9984	0.9828	0.9889	0.9907	0.9984
Functionalized	AIC	58.6869	74.78	84.67	64.98	42.85
Silymarin	MSC	4.0483	2.70	1.88	3.52	5.36
Loaded MSN						

Fig. 6. DSC thermograph of A. Silymarin, B. Silymarin loaded MSN, C. APTES functionalized Silymarin Loaded MSN

respectively. Particle size decreased in APTES functionalized Silymarin Loaded MSN because of stirring during drug loading. Data given for APTES functionalized Silymarin Loaded MSN in Figure 7.

In vitro dissolution study

The release profile of Silymarin loaded MSN, Surface functionalized silymarin loaded MSNs, by taking different concentrations of
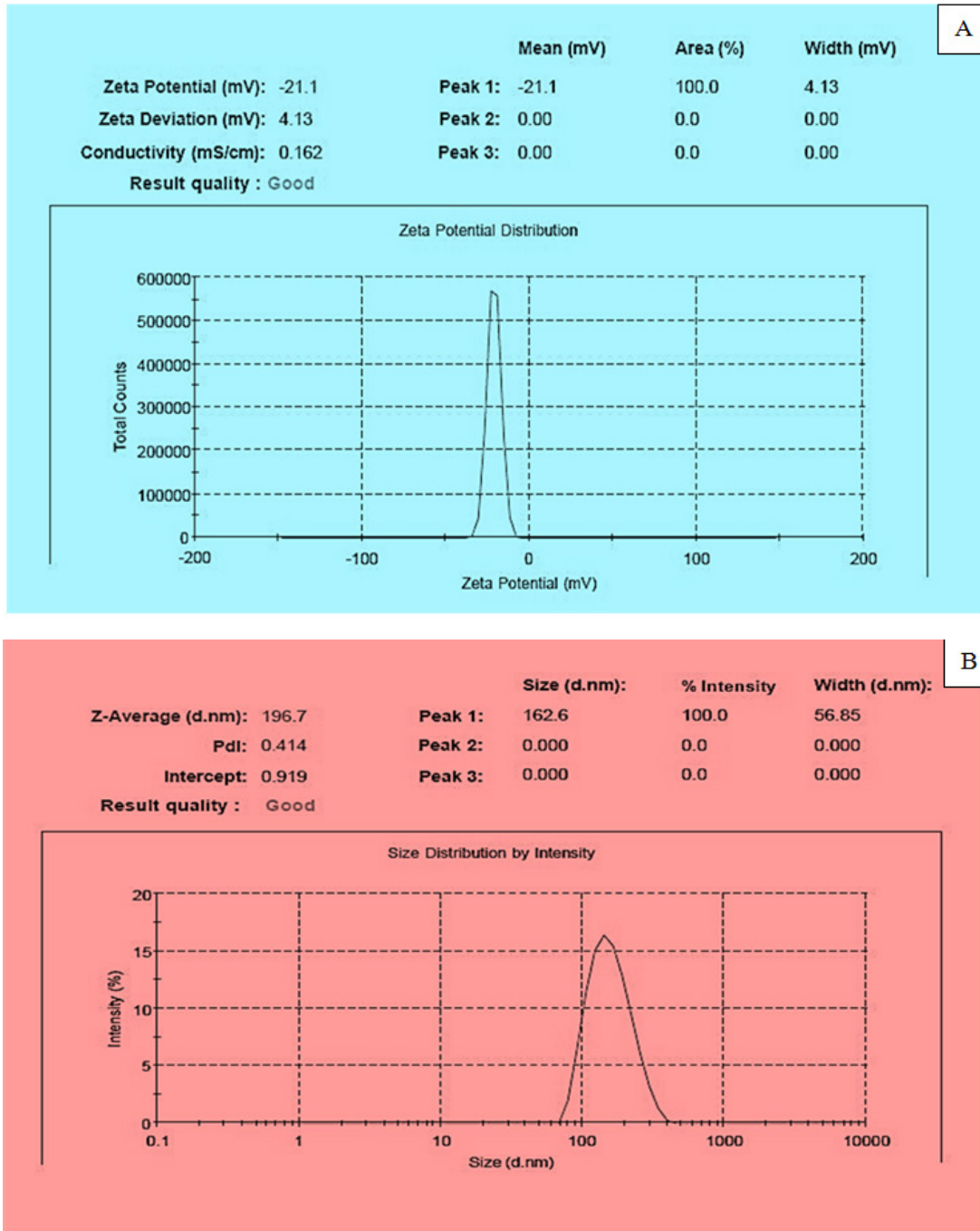
Fig. 7. A) Zeta potential of APTES Functionalized Silymarin Loaded MSN B) Particle size of APTES Functionalized Silymarin Loaded MSN

APTES at pH 7.4 for 12 hrs. Initially their release of drug in Silymarin Loaded MSN 3.75% and maximum drug release 79.25% at the end of 12 hrs. Result showed the release of silymarin from Amino-functionalized silymarin loaded MSN, initially burst release 14.14 % at 1 h followed by 92.15±0.03% release at 12h for the optimized batch. The initial burst release was due to the drug being absorbed on the surface of particles. The drug initially occupied the large internal surface of pores, when it was covered; the drug formed a thin film over an external surface. The slow release
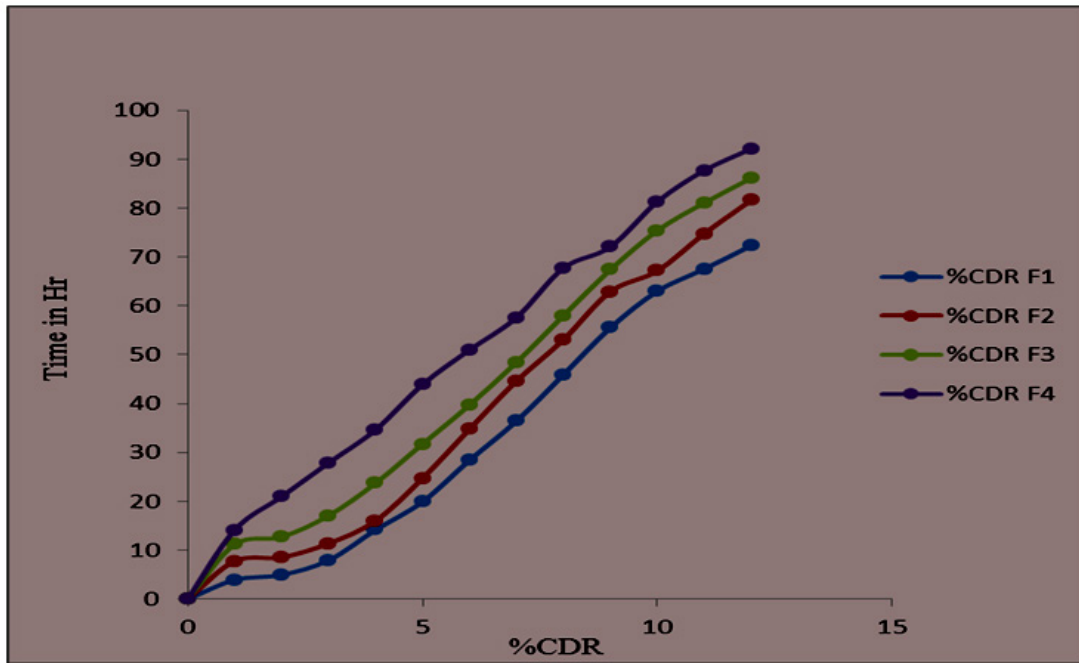

Fig. 8. Cumulative drug release (CDR) of Amino functionalized MSN at various concentration of APTES. F1) 0.5 % F2) 1% F3) 1.5% F4) 2%
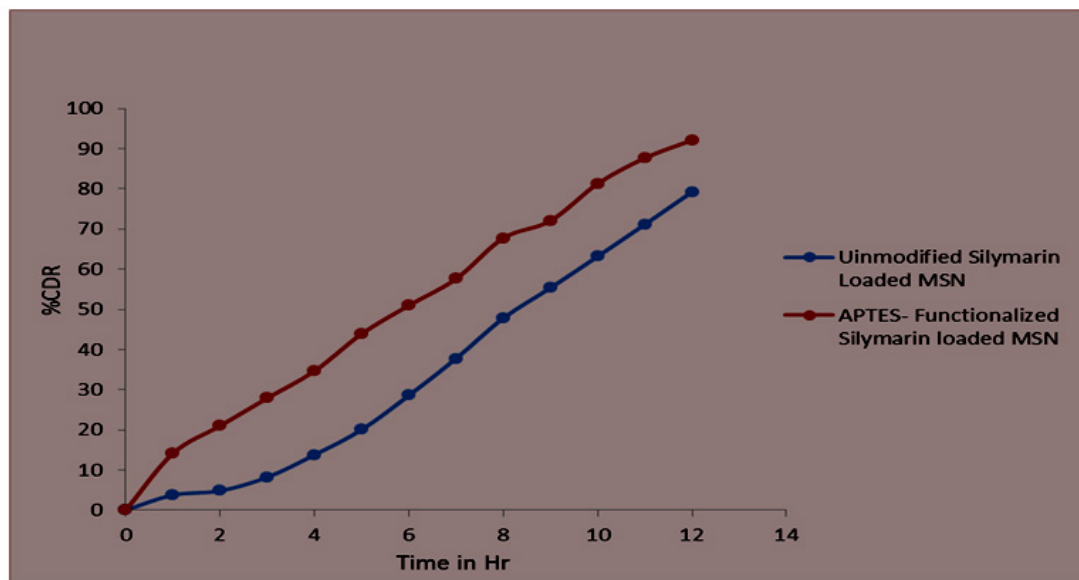

Fig. 9. In vitro dissolution study of Silymarin Loaded MSN and APTES functionalized Silymarin Loaded MSN

was observed due to the excess of overloaded drugs blocking the pores and hindering the release. The highest release was found in batch F4, due to more concentration of APTES (2%) shown in Figure 7 and 8. The highest release of surface functionalized silymarin loaded MSN as compared to silymarin loaded MSN (without surface functionalization) because of interaction between silanol group and $-Si-O_2$ $-NH_2$ in APTES, so more energy is required to break these bonds. Furthermore, the collected percent cumulative drug release (%CDR) values were subjected to a variety of dissolution kinetic models. In the cases of Silymarin loaded MSN and amino functionalized Silymarin loaded MSN, the model with the greatest regression coefficient, MSC value, and lowest AIC criterion was the best fit. Korsmeyer Peppas model was found to be the best fit satisfying all three criteria (Table 5, 6).

CONCLUSION

The drug was adsorbed on the surface of pore as well as inside, according to the examination of silica particles. By increasing surface area, pore size, and pore volume, the drug's transformation from crystalline to amorphous form and the use of mesoporous silica nanoparticles as a carrier improved silymarin dissolution. However, the findings reveal that the rate of Silymarin dissolution is influenced by the exterior chemical component of MSNs. The amine groups on the surface of APTES Functionalized Silymarin loaded MSN and the carboxyl groups of Silymarin may interact ionically to influence the release rate of Silymarin from functionalized MSNs. We believe that the current study may help to design oral drug delivery systems that enhance the dissolution and/or delayed release of poorly water-soluble drugs.

ACKNOWLEDGEMENTS

Conflict of Interest

The author declares that they do not have any conflict of interests

Funding Sources

Data Availability Statement

This statement does not apply to this article.

Ethic Approval

This research did not involve human participants, animal subjects, or any material that requires ethical approval.

Authors Contribution

Sheetal B. Gosavi: Contributed equally.; Moreshwar P. Patil: Contributed equally

REFERENCES

1. Beig, A., Miller, J. M., & Dahan, A. (2012). Accounting for the solubility–permeability interplay in oral formulation development for poor water solubility drugs: the effect of PEG-400 on carbamazepine absorption. *European Journal of Pharmaceutics And Biopharmaceutics*, *81*(2), 386-391.

2. Kalepu, S., & Nekkanti, V. (2015). Insoluble drug delivery strategies: review of recent advances and business prospects. *Acta Pharmaceutica Sinica B*, *5*(5), 442-453.

3. Kesisoglou, F., Panmai, S., & Wu, Y. (2007). Nanosizing—oral formulation development and biopharmaceutical evaluation. *Advanced Drug Delivery Reviews*, *59*(7), 631-644.

4. Lipinski, C. A. L. F. (2002). Poor aqueous solubility—an industry wide problem in drug discovery. *Am. Pharm. Rev*, *5*(3), 82-85.

5. Mishra, B., Sahoo, J., & Dixit, P. K. (2016). Enhanced bioavailability of cinnarizine nanosuspensions by particle size engineering: Optimization and physicochemical investigations. *Materials Science and Engineering: C*, *63*, 62-69.

6. Vasconcelos, T., Sarmento, B., & Costa, P. (2007). Solid dispersions as strategy to improve oral bioavailability of poor water soluble drugs. *Drug Discovery Today*, *12*(23-24), 1068-1075.

7. Wong, S. M., Kellaway, I. W., & Murdan, S. (2006). Enhancement of the dissolution rate and oral absorption of a poorly water soluble drug by formation of surfactant-containing microparticles. *International Journal of Pharmaceutics*, *317*(1), 61-68.

8. Sachs-Barrable, K., Lee, S. D., Wasan, E. K., Thornton, S. J., & Wasan, K. M. (2008).

Enhancing drug absorption using lipids: a case study presenting the development and pharmacological evaluation of a novel lipid-based oral amphotericin B formulation for the treatment of systemic fungal infections. *Advanced Drug Delivery Reviews*, *60*(6), 692-701.

9. Vallet-Regi, M., Rámila, A., Del Real, R. P., & Pérez-Pariente, J. (2001). A new property of MCM-41: drug delivery system. *Chemistry of Materials*, *13*(2), 308-311.

10. Tasciotti, E., Liu, X., Bhavane, R., Plant, K., Leonard, A. D., Price, B. K.,& Ferrari, M. (2008). Mesoporous silicon particles as a multistage delivery system for imaging and therapeutic applications. *Nature Nanotechnology*, *3*(3), 151-157.

11. Van Speybroeck, M., Barillaro, V., Do Thi, T., Mellaerts, R., Martens, J., Van Humbeeck, J.,& Augustijns, P. (2009). Ordered mesoporous silica material SBA-15: a broad-spectrum formulation platform for poorly soluble drugs. *Journal of pharmaceutical sciences*, *98*(8), 2648-2658.

12. Kilpeläinen, M., Riikonen, J., Vlasova, M. A., Huotari, A., Lehto, V. P., Salonen, J., & Järvinen, K. (2009). In vivo delivery of a peptide, ghrelin antagonist, with mesoporous silicon microparticles. *Journal of Controlled Release*, *137*(2), 166-170.

13. Li, Z. Z., Wen, L. X., Shao, L., & Chen, J. F. (2004). Fabrication of porous hollow silica nanoparticles and their applications in drug release control. *Journal of Controlled Release*, *98*(2), 245-254.

14. Cao, L., Man, T., & Kruk, M. (2009). Synthesis of ultra-large-pore SBA-15 silica with two-dimensional hexagonal structure using triisopropylbenzene as micelle expander. *Chemistry of Materials*, *21*(6), 1144-1153.

15. He, Q., Zhang, J., Shi, J., Zhu, Z., Zhang, L., Bu, W., & Chen, Y. (2010). The effect of PEGylation of mesoporous silica nanoparticles on nonspecific binding of serum proteins and cellular responses. *Biomaterials*, *31*(6), 1085-1092.

16. Vivero-Escoto, J. L., Slowing, I. I., & Lin, V. S. Y. (2010). Tuning the cellular uptake and cytotoxicity properties of oligonucleotide intercalator-functionalized mesoporous silica nanoparticles with human cervical cancer cells HeLa. *Biomaterials*, *31*(6), 1325-1333.

17. Zhao, D., Feng, J., Huo, Q., Melosh, N., Fredrickson, G. H., Chmelka, B. F., & Stucky, G. D. (1998). Triblock copolymer syntheses of mesoporous silica with periodic 50 to 300 angstrom pores. *Science*, *279*(5350), 548-552.

18. Kresge, A. C., Leonowicz, M. E., Roth, W. J., Vartuli, J. C., & Beck, J. S. (1992). Ordered mesoporous molecular sieves synthesized by a liquid-crystal template mechanism. *Nature*, *359*(6397), 710-712..

19. Lee, C. H., Lin, T. S., & Mou, C. Y. (2009). Mesoporous materials for encapsulating enzymes. *Nano Today*, *4*(2), 165-179.

20. Slowing, I. I., Vivero-Escoto, J. L., Wu, C. W., & Lin, V. S. Y. (2008). Mesoporous silica nanoparticles as controlled release drug delivery and gene transfection carriers. *Advanced Drug Delivery Reviews*, *60*(11), 1278-1288.

21. Huang, X., Teng, X., Chen, D., Tang, F., & He, J. (2010). The effect of the shape of mesoporous silica nanoparticles on cellular uptake and cell function. *Biomaterials*, *31*(3), 438-448.

22. Salonen, J., Laitinen, L., Kaukonen, A. M., Tuura, J., Björkqvist, M., Heikkilä, T., ... & Lehto, V. P. (2005). Mesoporous silicon microparticles for oral drug delivery: loading and release of five model drugs. *Journal of Controlled Release*, *108*(2-3), 362-374.

23. Song, S. W., Hidajat, K., & Kawi, S. (2005). Functionalized SBA-15 materials as carriers for controlled drug delivery: influence of surface properties on matrix" drug interactions. *Languir*, *21*(21), 9568-9575.

24. Chen, J. F., Ding, H. M., Wang, J. X., & Shao, L. (2004). Preparation and characterization of porous hollow silica nanoparticles for drug delivery application. *Biomaterials*, *25*(4), 723-727.

25. Nandiyanto, A. B. D., Kim, S. G., Iskandar, F., & Okuyama, K. (2009). Synthesis of spherical mesoporous silica nanoparticles with nanometer-size controllable pores and outer diameters. *Microporous and Mesoporous Materials*, *120*(3), 447-453.

26. Vazquez, N. I., Gonzalez, Z., Ferrari, B., & Castro, Y. (2017). Synthesis of mesoporous silica nanoparticles by sol–gel as nanocontainer for future drug delivery applications. *Boletín de la Sociedad Española de Cerámica y Vidrio*, *56*(3), 139-145.

27. Wang, S. (2009). Ordered mesoporous materials for drug delivery. *Microporous and Mesoporous Materials*, *117*(1-2), 1-9.

28. Kilpeläinen, M., Riikonen, J., Vlasova, M. A., Huotari, A., Lehto, V. P., Salonen, J., & Järvinen, K. (2009). In vivo delivery of a peptide, ghrelin antagonist, with mesoporous silicon microparticles. *Journal of Controlled Release*, *137*(2), 166-170.

29. Zhang, Y., Zhi, Z., Jiang, T., Zhang, J., Wang, Z., & Wang, S. (2010). Spherical mesoporous

silica nanoparticles for loading and release of the poorly water-soluble drug telmisartan. *Journal of Controlled Release*, *145*(3), 257-263.

30. El-Samaligy, M. S., Afifi, N. N., & Mahmoud, E. A. (2006). Increasing bioavailability of silymarin using a buccal liposomal delivery system: preparation and experimental design investigation. *International Journal of Pharmaceutics*, *308*(1-2), 140-148.

31. Vazquez, N. I., Gonzalez, Z., Ferrari, B., & Castro, Y. (2017). Synthesis of mesoporous silica nanoparticles by sol–gel as nanocontainer for future drug delivery applications. *Boletín de la Sociedad Española de Cerámica y Vidrio*, *56*(3), 139-145.

32. Li, Z., Zhang, Y., & Feng, N. (2019). Mesoporous silica nanoparticles: synthesis, classification, drug loading, pharmacokinetics, biocompatibility, and application in drug delivery. *Expert Opinion on Drug Delivery*, *16*(3), 219-237.

33. Zhang, Y., Zhi, Z., Jiang, T., Zhang, J., Wang, Z., & Wang, S. (2010). Spherical mesoporous silica nanoparticles for loading and release of the poorly water-soluble drug telmisartan. *Journal of Controlled Release*, *145*(3), 257-263.